

Synthesis of Carbon Supported Pd-Sn Catalysts by Ethylene Glycol Method for Ethanol Electrooxidation

Yunhua Li¹, Yajun Wang¹, Hongmin Mao², Qiaoxia Li^{1,*}

¹ Shanghai Key Laboratory of Materials Protection and Advanced Materials in Electric Power, College of Environmental and Chemical Engineering, Shanghai University of Electric Power, 2103 Pingliang Road, Yangpu District, Shanghai, 200090, China

² Wuhan Product Quality Supervision & Testing institute, No.5 Donger Road, Jinyin Lake, Dongxihu District, Wuhan, Hubei, 430048, China

*E-mail: liqiaoxia@shiep.edu.cn

Received: 4 April 2016 / *Accepted:* 26 May 2016 / *Published:* 7 July 2016

Carbon supported Pd-Sn catalysts (Pd-Sn/C-EG) were synthesized by an ethylene glycol method. The resulting catalysts exhibited high electrical catalytic activity for ethanol oxidation in alkaline solution. Transmission electron microscopy analysis was shown that the prepared Pd-Sn catalysts were uniformly dispersed on the carbon support with a mean particle size of 1.63 nm. X-ray diffraction patterns for all samples indicated a fcc crystalline structure. The negative shift observed for Pd (111) suggested that Sn could shrink the Pd crystalline lattice. The electrocatalytic activity and long-term stability towards ethanol electrooxidation of the Pd-Sn/C-EG catalyst were superior to that of a commercially available 20 wt.% Pd/C. More importantly, the oxidation peak current of the Pd-Sn/C-EG was found to be twice as large compared with that of Pd/C. This difference may be attributed to the uniform distribution of the prepared nanoparticles and the third body effect induced by addition of Sn onto the Pd surface. Furthermore, Sn doping can significantly provide the adsorption of OH species and speed up the ethanol oxidation reaction.

Keywords: ethanol electrooxidation; ethylene glycol method; Pd-based; Sn doping

1. INTRODUCTION

Recently, direct ethanol fuel cells (DEFCs) have received increased recognition as a clean and portable power source. Ethanol has several advantages, such as low toxicity, safe storage and transportation properties, high energy density (8.01 kW h⁻¹kg⁻¹), and renewable [1]. However, ethanol electrooxidation is a complex process, and exploitation of high activity anodic catalysts for DEFCs remains challenging. Although platinum is considered an ideal active component for ethanol

electrooxidation, it is readily poisoned by CO intermediates formed during the oxidation process [2, 3]. Palladium has also been considered as a candidate for DEFCs owing to its higher tolerance to poisoning in alkaline media and lower price than Pt [4, 5]. Thus, improving the catalytic activity and stability of Pd is a promising field of interest.

There has been extensive previous work into more efficient Pd-based catalysts. Alloy catalysts are under development, with the expectation that the less costly metal or nonmetal components may also promote the catalytic activity and stability. Many Pd-based bi- and tri-metallic nanoparticles, including Pd-Sn intermetallics in network nanostructures[6], Pd-Ag/C [7], and Pd-Ni-P/C [8], have been evaluated. PdNi/C, PdCu/C, and PdNiCu/C alloys have been previously synthesized by a one-step sodium hypophosphite reduction method [9], with results showing that PdNiCu/C alloys display the highest potential for formic acid electrochemical oxidation. In addition, nitrogen-doped grapheme supported PdSn catalysts have been synthesized via a facile chemical reaction with NaBH₄ as the reductant [2], which was shown to significantly improve the electrochemical performance with low Pd loading. Moderate amounts of Sn can also enhance the catalytic performance of Pd catalysts.

Mild reducing agents have been investigated for the preparation of highly active and stable Pd-based catalysts. Theoretical studies of traditional NaBH₄ reduction methods with Pd-Ni/MWCNT[10], Au/Pd bimetallic nanoparticles [11], Ag/Pd nanocomposites [12], Pd-Ru/C [13], and PdSnPt_x/C [13] have carried out. However, rapid NaBH₄ reductant methods result in aggregation of the Pd nanoparticles, which may decrease the active surface area available for reaction with the large particle size [14]. A previous study by Meixia Wu [15] showed that highly dispersed Pd/C electrocatalysts with a narrow size distribution can be prepared by a hydrogen gas reduction process. These catalysts were found to be highly electrocatalytic performance due to the high viscosity of ethylene glycol and the stabilizing effect of sodium citrate. While these results were promising, there is still a need to identify and evaluate highly active reducing agents. Ethylene glycol, for example, has been shown to be an ideal reductant and solvent [16].

In this study, carbon-supported Pd-Sn catalysts (Pd-Sn/C-EG) were synthesized through an ethylene glycol method. The catalysts were characterized by transmission electron microscopy (TEM) and X-ray diffraction (XRD), and also analyzed for ethanol electrooxidation in alkaline media by cyclic voltammetry and chronoamperometry.

2. EXPERIMENTAL

2.1 Materials

Vulcan XC-72 carbon black and 5 wt% Nafion solutions were purchased from Cabot Co. (Boston, MA, USA). Analytical grade ethanol (CH₃CH₂OH), Palladium chloride (PdCl₂), ethylene glycol (C₂H₆O₂), sodium hydroxide (NaOH), and stannous chloride dihydrate (SnCl₂·2H₂O) were purchased from Sinopharm Chemical Reagent Co. Ltd (SCRC, Shanghai, China). A commercial Pd/C catalyst (JM, 20 wt. % Pd) was purchased from the Johnson Matthey Company. All aqueous solutions were prepared in ultrapure water (> 18.2MΩ) from a Milli-Q Plus system (Millipore).

2.2 Preparation of Pd-Sn/C-EG

The Pd-Sn/C-EG was prepared as follows. A given amount of $\text{SnCl}_2 \cdot 2\text{H}_2\text{O}$ was dispersed in 10 mL ethylene glycol and sonicated for several minutes, after which 40 mL of ethylene glycol was slowly poured into the suspension. The mixture was heated in an oil bath and stirred at a constant temperature of 190°C for 2 h and then cooled to room temperature. PdCl_2 (16.7 mg) and an appropriate amount of sodium citrate were dissolved in 10 mL ethylene glycol before dropwise into the above mixture. After heating at $70\text{--}80^\circ\text{C}$ for 2 h, 20 mg of acid-pretreated Vulcan XC-72 carbon black was added to the mixture and the pH of the reaction system was adjusted to ca. 12 with 5 wt% NaOH solution. The suspension was stirred for another 2 h at 130°C and then filtered, washed with ultrapure Milli-Q water, and vacuum dried overnight at 60°C .

Pd/C and Sn/C were prepared by the same method, except that SnCl_2 and PdCl_2 were absent, respectively. A commercial Pd/C catalyst (Johnson-Matthey, 20 wt % Pd) served as the reference sample.

2.3 Catalyst characterization

The morphology and dispersity of the as-prepared Pd-based catalysts were characterized by TEM/EDS (JEOL 2100F). X-ray diffraction (XRD) for Pd-Sn/C-EG was performed using a Bruker D8-Advance X-ray diffractometer (Karlsruhe, Germany) with $\text{Cu } \alpha$ radiation ($\lambda = 0.15406 \text{ nm}$).

2.4 Electrochemical measurements

Cyclic voltammetry and chronoamperometry were carried out at room temperature with a CHI660A electrochemistry workstation (CH Instruments, Shanghai Chenhua, Shanghai, China) in a conventional three-electrode cell. A Pt foil and a saturated calomel electrode (SCE) served as the counter electrode and reference electrode, respectively. The working electrode was prepared as follows. The catalyst ink was prepared by dispersing 2 mg of catalyst sample in 800 μL of alcohol containing 200 μL of water and 120 μL of Nafion solution (5 wt. %) under sonication. An aliquot of catalyst ink (5.6 μL) was transferred on a glassy carbon electrode ($\Phi = 3 \text{ mm}$) with a Pd loading of 28 $\mu\text{g}\cdot\text{cm}^{-2}$.

3. RESULTS AND DISCUSSION

The TEM images for Pd-Sn/C-EG and Pd/C catalysts were shown in Fig. 1A and B, respectively. TEM results showed that the catalytic nanoparticles were uniformly dispersed on the surfaces of carbon supports, and that the particles had a narrow size range, with a mean diameter of 1.63 nm. While, Pd/C catalysts ranged in size from 2 to 11 nm, with a mean diameter of 5.92 nm. The particle size distribution was shown as an inset in Fig 1. The size difference between Pd-Sn/C-EG and Pd/C may be attributed to the influence of high viscosity of ethylene glycol on the distribution of

catalyst as solvent and reducing agent [15-18]. The EDS spectra of the Pd-Sn/C-EG catalyst (Fig 2) showed the presence of Sn besides Pd and C, indicating that Pd/C catalysts doped with Sn were successfully synthesized by the ethylene glycol method.

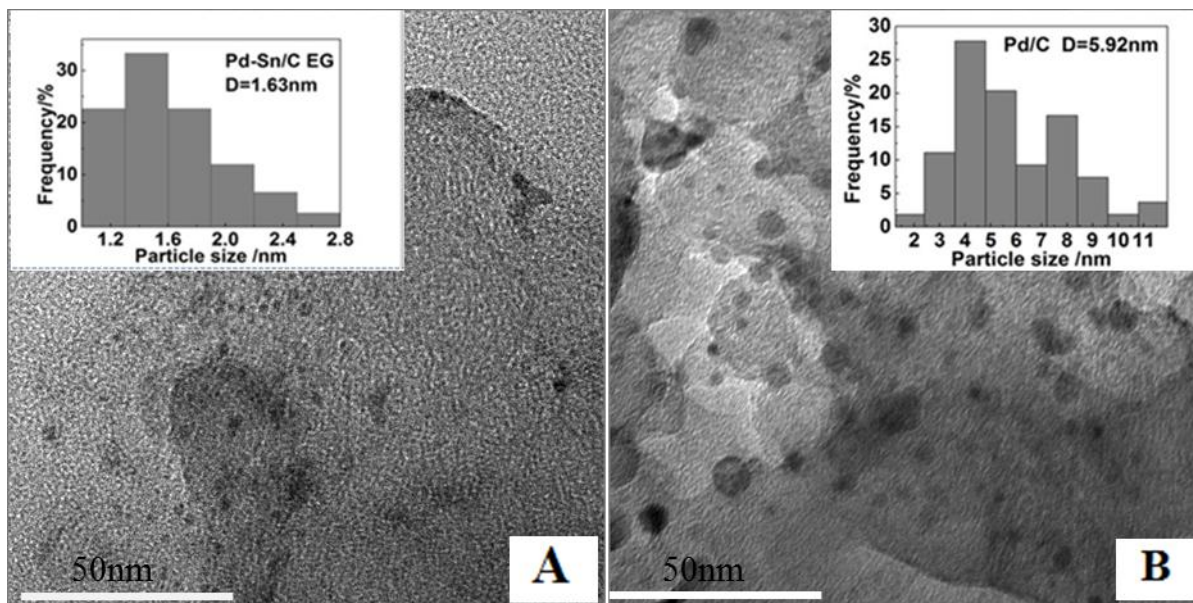


Figure 1. TEM images and their corresponding particle size distribution histogram: (A) Pd-Sn/C-EG, (B) Pd/C catalysts.

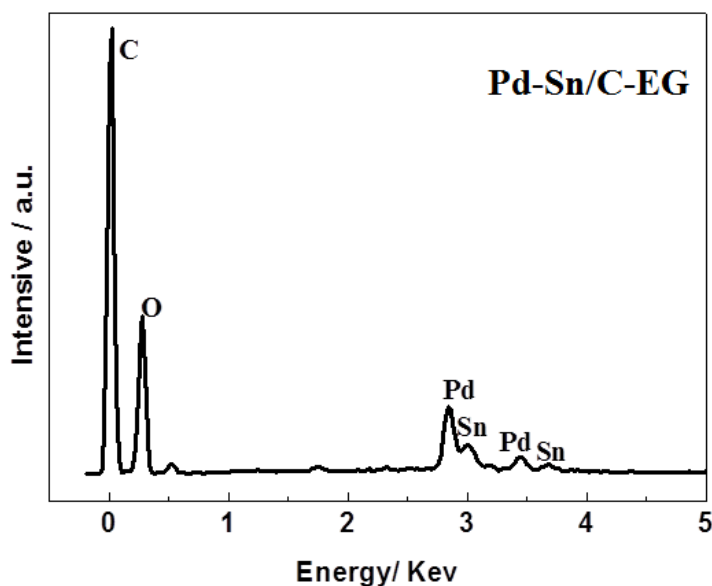


Figure 2. EDS spectrum of the Pd-Sn/C-EG catalyst.

XRD patterns of the Pd-Sn/C-EG and Pd/C catalysts were shown in Fig 3. All samples displayed a peak located at ca. 26° (2θ) which corresponded to the hexagonal structure of the Vulcan

XC-72 carbon black support. The main diffraction peaks for the Pd/C catalyst at 40.06° , 46.68° , 68.08° , 82.08° , and 86.60° were characteristic peaks of Pd(111), (200), (220), (311), (222) planes, respectively, which suggested Pd exists in a face-centered cubic structure. In addition, diffraction peaks observed at ca. 39.70° , 46.48° , 68.15° can be attributed to Pd₃Sn alloy phase diffraction peaks of the (111), (200), and (220) crystal faces, respectively. In general, compared with Pd-Sn/C-EG and Pd/C, the characteristic peaks of Pd-Sn/C-EG slightly but consistently observed at lower 2θ values. These results suggested the formation of a Pd-Sn alloy phase between Pd and Sn caused by the incorporation of Sn atoms into the fcc structure of Pd [19, 20]. XRD analysis also showed broadening of the Pd(111) diffraction peak for Pd-Sn/C-EG, demonstrating that the catalyst nanoparticles were smaller in particle size [21]. The XRD results were consistent with the results of TEM analysis.

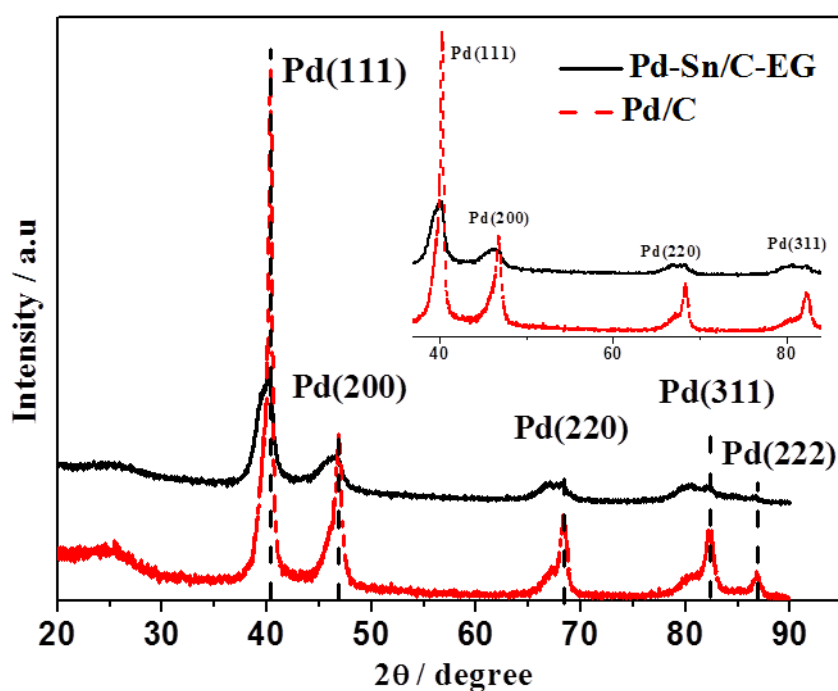


Figure 3. XRD patterns of the Pd-Sn/C-EG, Pd/C.

The electrocatalytic activity of the synthesized catalysts for ethanol oxidation was investigated by cyclic voltammetry (CV) and chronoamperometry (CA) as shown in Fig. 4, Fig. 5 and Fig. 6. The CV results for Pd-Sn/C-EG, Pd/C, Sn/C, and Pd/C (JM) in 1.0 M KOH solution were shown in Fig. 4. The CV curves exhibited well-defined peaks in the hydrogen adsorption/desorption region (-1.0 — -0.6 V), as well as cathodic peaks near -0.45 V for the reduction of Pd-O(H) species. Hydrogen adsorption/desorption peaks can be used to calculate the electrochemical surface area (ECSA) [22, 23]. The ECSAs for the Pd-Sn/C-EG, Pd/C, and Pd/C (JM) catalysts were 27.47 m²/g, 10.40 m²/g, and 12.53 m²/g, respectively, which indicated that the Pd-Sn/C-EG catalyst possessed the highest electrocatalytic activity. The CVs for the electrooxidation of ethanol in a 1.0 mol/L KOH containing

1.0 mol/L C_2H_5OH aqueous solution on the three catalysts are shown in Fig. 5. Compared to the Pd/C catalyst, the onset potential (E_{op}) of Pd-Sn/C-EG were shifted toward a negative direction.

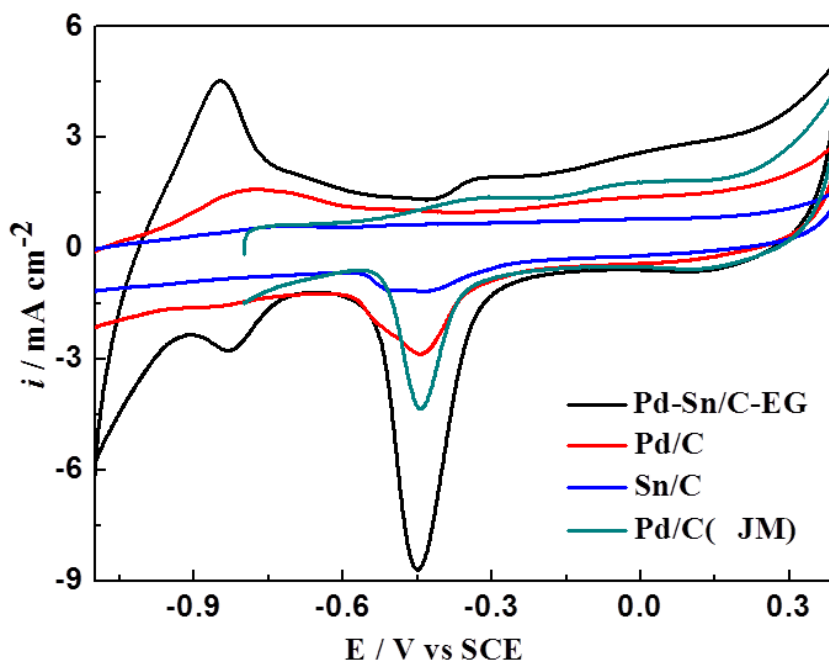


Figure 4. Cyclic voltammograms of the Pd-Sn/C-EG, Pd/C, Sn/C and Pd/C (JM) catalysts in $1.0 \text{ mol}\cdot\text{L}^{-1}$ KOH at $50 \text{ mV}\cdot\text{s}^{-1}$ scan rate.

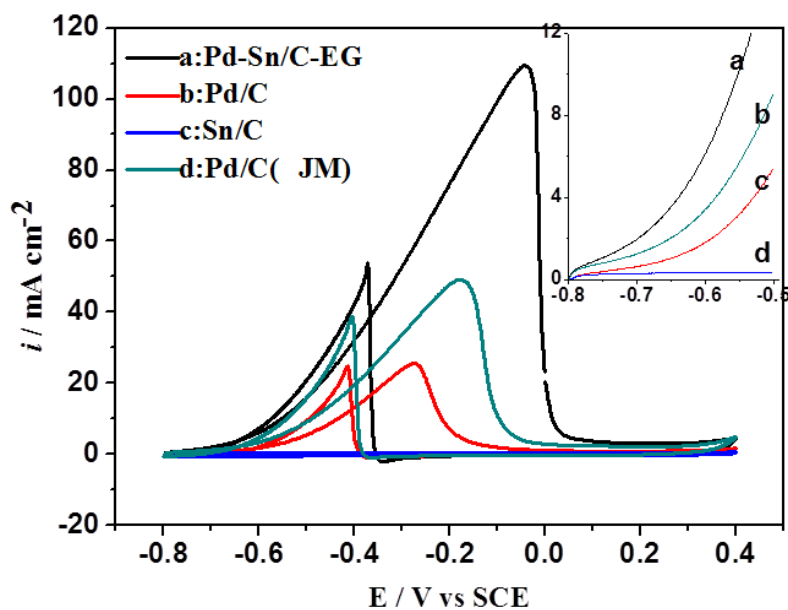


Figure 5. Cyclic voltammogram curves of the Pd-Sn/C-EG, Pd/C, Sn/C, and Pd/C (JM) catalysts in $1.0 \text{ mol}\cdot\text{L}^{-1}$ KOH + $1.0 \text{ mol}\cdot\text{L}^{-1}$ C_2H_5OH aqueous solution, The insert figure shows the enlarged parts in the potential range of $-0.8 \text{ V} \sim -0.5 \text{ V}$ in the positive scan. The scan rate of potential was $50 \text{ mV}\cdot\text{s}^{-1}$.

As shown in this pattern, bare SnO_2/C nanoparticles without Pd displayed had no current response for ethanol oxidation [24, 25]. Furthermore, the ethanol oxidation peak current density (i_p) on Pd-Sn/C-EG ($109.39 \text{ mA}\cdot\text{cm}^{-2}$) was found to be 4.27 times higher than that of Pd/C ($25.6 \text{ mA}\cdot\text{cm}^{-2}$), and 2.23 times higher than that of Pd/C (JM) ($49.16 \text{ mA}\cdot\text{cm}^{-2}$). These observations indicate that Pd-Sn/C-EG synthesized by the ethylene glycol method results in higher electrocatalytic activity [26] which can be attributed to the weakened adsorption of the CO intermediate produced during ethanol oxidation with the addition of Sn creating more active Pd sites for further ethanol oxidation. Ethylene glycol acts as an effective solvent and reducing agent, allowing for homogeneous distribution of Pd nanoparticles on the support and improving the utilization of noble metal.

In order to garner more information about the electrocatalytic stability of the catalysts, chronoamperometric measurements were performed at -0.3V vs. SCE (Fig. 6). A sharp decrease in the current density during the initial stage was observed in the chronoamperometry curves. Pd-Sn/C-EG was found to display the highest current density among three catalysts. The results of chronoamperometric measurements at 100s, 1000s, 3600s were summarized in the insert of Fig. 6. The current density at 1000s on the Pd-Sn/C-EG was found to be $35 \text{ mA}\cdot\text{cm}^{-2}$, more than 5 times higher than that on the Pd/C (JM) catalyst. The current densities at 3600s were $13.91 \text{ mA}\cdot\text{cm}^{-2}$ for Pd-Sn/C-EG, $0.64 \text{ mA}\cdot\text{cm}^{-2}$ for Pd/C, and $3.07 \text{ mA}\cdot\text{cm}^{-2}$ for Pd/C (JM), respectively. These results indicated that the stability of the catalyst followed the order Pd-Sn/C-EG > Pd/C (JM) > Pd/C. These results, combined with the cyclic voltammetry (CV) tests above, confirmed the high electrocatalytic stability and activity of Pd-Sn/C-EG for electrooxidation of ethanol. These results also indicated that the presence of Sn provides OH_{ads} , which sped up the oxidation of the adsorbed alcohols.

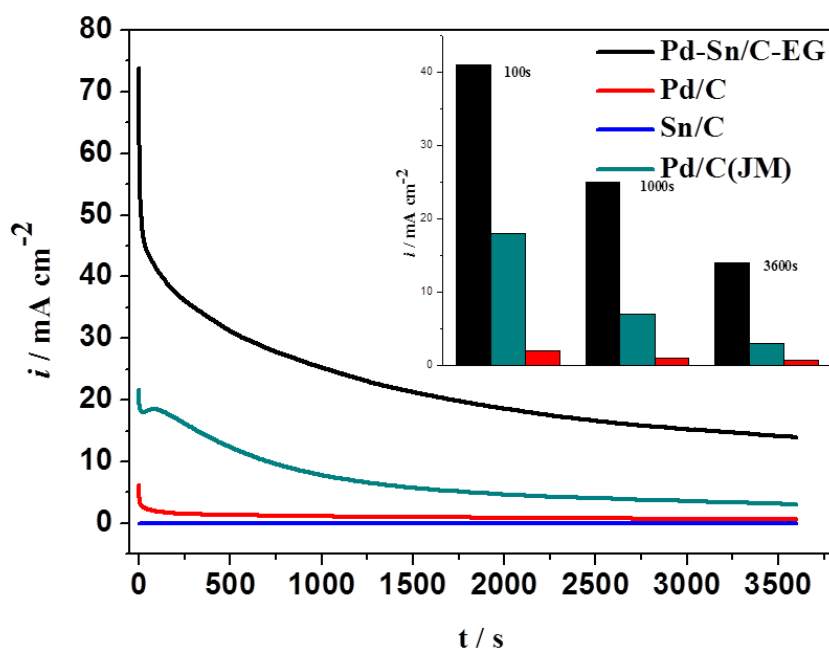


Figure 6. Chronoamperometry curves for ethanol oxidation in $1.0 \text{ mol}\cdot\text{L}^{-1}$ KOH and $1.0 \text{ mol}\cdot\text{L}^{-1}$ $\text{C}_2\text{H}_5\text{OH}$ on the Pd-Sn/C-EG, Pd/C, Sn/C, and Pd/C (JM) at -0.30 V .

The physicochemical properties and electrochemical characterization of commercially available Pd/C (JM), Pd/C, and Pd-Sn/C-EG catalysts for ethanol electrooxidation were listed in Table 1. The samples prepared in the current study were capable of accelerating the oxidation of ethanol. Generally, this acceleration in oxidation is derived from two effects: 1) Improvements in the distribution nanoparticles, and optimal nanoparticle size due to the high viscosity of ethylene glycol; 2) The third body effect due to the addition of Sn which provides –OH groups and thus remove poisoning species from the catalytic surface.

Table 1. Physicochemical properties and electrochemical characterization of Pd/C (JM), Pd/C and Pd-Sn/C-EG catalysts for ethanol electrooxidation.

Catalyst	Crastallitesize(nm) ^a	ECSA (m ² ·g ⁻¹) ^b	i _p (mA·cm ⁻²) ^c	E _{op} (V) ^d
Pd/C (JM)	-	12.53	49.16	-0.72
Pd/C	5.92	10.40	25.6	-0.68
Pd-Sn/C-EG	1.63	27.47	109.39	-0.78

^aMeasured by the Transmission electron microscopy (TEM).

^{b c d}Measured by the cyclic voltammetry (CV).

4. CONCLUSIONS

Carbon supported Pd-Sn catalysts were prepared using an ethylene glycol method. The as-prepared Pd-Sn/C-EG exhibited superior catalytic activity and stability for electrooxidation of ethanol in alkaline medium compared with home-made Pd/C and commercially available Pd/C (JM). Findings from this study also show that ethylene glycol is an effective solvent and reducing agent, which can improve the dispersity of catalysts for energy transfer fields.

ACKNOWLEDGEMENTS

This work was financially supported by the Natural Science Foundation of China (21103107), Key Project of Shanghai Committee of Science and Technology, China (10160502300), Science and Technology Commission of Shanghai Municipality (No: 14DZ2261000).

References

1. Q. Wang, G.Q. Sun, L. Cao, L.H. Jiang, G.X. Wang, S.L. Wang, S.H. Yang, Q. Xin, *Journal of Power Sources*, 177 (2008) 142.
2. Y. Feng, D. Bin, K. Zhang, F. Ren, J. Wang, Y. Du, *RSC Adv.*, 6 (2016) 19314.
3. A. Oliveira Neto, M. Brandalise, R.R. Dias, J.M.S. Ayoub, A.C. Silva, J.C. Pentead, M. Linardi, E.V. Spinacé, *International Journal of Hydrogen Energy*, 35 (2010) 9177.
4. J. Liu, J. Ye, C. Xu, S.P. Jiang, Y. Tong, *Electrochemistry Communications*, 9 (2007) 2334.

5. J. Wang, H. Chen, Z. Hu, M. Yao, Y. Li, *Catalysis Reviews*, 57 (2014) 79.
6. D. Sun, L. Si, G. Fu, C. Liu, D. Sun, Y. Chen, Y. Tang, T. Lu, *Journal of Power Sources*, 280 (2015) 141.
7. Y. Yang, W. Wang, Y. Liu, F. Wang, Z. Zhang, Z. Lei, *International Journal of Hydrogen Energy*, 40 (2015) 2225.
8. Y. Wang, F.-F. Shi, Y.-Y. Yang, W.-B. Cai, *Journal of Power Sources*, 243 (2013) 369.
9. S. Hu, F. Munoz, J. Noborikawa, J. Haan, L. Scudiero, S. Ha, *Applied Catalysis B: Environmental*, 180 (2016) 758.
10. Q. Yi, Q. Chen, *Electrochimica Acta*, 182 (2015) 96.
11. S. Tokonami, H. Zhang, Y. Cao, L. Lu, Z. Cheng, S. Zhang, *Journal of Nanoscience and Nanotechnology*, 15 (2015) 5785.
12. J. Liu, L. Lan, R. Li, X. Liu, C. Wu, *International Journal of Hydrogen Energy*, 41 (2016) 951.
13. M.S. Wei, F.Q. Liu, *Int. J. Electrochem. Sci.*, 11 (2016) 2185.
14. X. Wang, F. Zhu, Y. He, M. Wang, Z. Zhang, Z. Ma, R. Li, *J Colloid Interface Sci*, 468 (2016) 200.
15. M. Wu, M. Li, X. Wu, Y. Li, J. Zeng, S. Liao, *Journal of Power Sources*, 294 (2015) 556.
16. H. Yu, Y. Zhu, H. Yang, K. Nakanishi, K. Kanamori, X. Guo, *Dalton transactions*, 43 (2014) 12648.
17. Z. Zhang, L. Xin, K. Sun, W. Li, *International Journal of Hydrogen Energy*, 36 (2011) 12686.
18. P.S. Fernández, D.S. Ferreira, C.A. Martins, H.E. Troiani, G.A. Camara, M.E. Martins, *Electrochimica Acta*, 98 (2013) 25.
19. Q. Yi, H. Chu, Q. Chen, Z. Yang, X. Liu, *Electroanalysis*, 27 (2015) 388.
20. M. Nakamura, R. Imai, N. Otsuka, N. Hoshi, O. Sakata, *The Journal of Physical Chemistry C*, 117 (2013) 18139.
21. Z. Zhang, J. Ge, L. Ma, J. Liao, T. Lu, W. Xing, *Fuel Cells*, 9 (2009) 114.
22. Q. Wang, Y. Liao, H. Zhang, J. Li, W. Zhao, S. Chen, *Journal of Power Sources*, 292 (2015) 72.
23. H. Mao, L. Wang, P. Zhu, Q. Xu, Q. Li, *International Journal of Hydrogen Energy*, 39 (2014) 17583.
24. X. Zhang, H. Zhu, Z. Guo, Y. Wei, F. Wang, *International Journal of Hydrogen Energy*, 35 (2010) 8841.
25. Z. Wen, S. Yang, Y. Liang, W. He, H. Tong, L. Hao, X. Zhang, Q. Song, *Electrochimica Acta*, 56 (2010) 139.
26. C. Mahendiran, T. Maiyalagan, K. Scott, A. Gedanken, *Materials Chemistry and Physics*, 128 (2011) 341.